Electromagnetic transition probabilities in the natural-parity rotational bands of ^{155,157}Gd

H. Kusakari,[1] M. Oshima,[2] A. Uchikura,[1] M. Sugawara,[3] A. Tomotani,[1]
S. Ichikawa,[2] H. Iimura,[2] T. Morikawa,[2,4] T. Inamura,[5]
and M. Matsuzaki[6]

[1] *Chiba University, Yayoi-cho, Inage-ku, Chiba 263, Japan*
[2] *Japan Atomic Energy Research Institute, Tokai, Naka, Ibaraki 319-11, Japan*
[3] *Chiba Institute of Technology, Shibazono, Narashino-shi, Chiba 275, Japan*
[4] *Hiroshima University, Kagamiyama, Higashi-hiroshima 724, Japan*
[5] *RIKEN, Cyclotron Laboratory, Wako-shi, Saitama 351-01, Japan*
[6] *Fukuoka University of Education, Akama, Munakata-shi, Fukuoka 811-41, Japan*

(Received 9 March 1992)

The ground-state rotational bands of ^{155}Gd and ^{157}Gd have been investigated through multiple Coulomb excitation with beams of 240-MeV ^{58}Ni and 305-MeV ^{81}Br. Gamma-ray branchings and $E2/M1$ mixing ratios were determined by γ-ray angular-distribution measurement. Nuclear lifetimes of levels up to $I = \frac{21}{2}$ and $\frac{23}{2}$ for ^{155,157}Gd, respectively, have been measured using the Doppler-shift recoil-distance method. The observed signature dependence of $M1$ transition rates was found to be inverted in relation to the quasiparticle energy splitting. The data are analyzed in terms of the cranking model.

PACS number(s): 23.20.−g, 27.70.+q, 25.70.Bc

I. INTRODUCTION

We have previously reported signature dependence of $M1$ strength in the natural-parity rotational band of ^{163}Dy [1,2]. This has drawn considerable attention since the signature dependence is unexpectedly large and the phase of the zigzag pattern as a function of spin contradicts the selection rule [3] that is well established for unique-parity rotational bands based on high-j orbits [4–10]: While the sign of quasiparticle energy splitting, $\Delta e' = e'_{+i} - e'_{-i}$, and the averaged absolute value of $B(M1)$ are in agreement with the dominant $j = \frac{9}{2}$ character for this band, the phase of the zigzag contradicts that expected for the dominant $j = \frac{9}{2}$ configuration [1,2]; we for the first time pointed out this unexpected zigzag pattern of $B(M1)$ as the "inverted" signature dependence. The signature dependence was shown in terms of the cranking model (previously referred to as "the rotating shell model") to originate from the characteristic coherence between the orbital and spin contributions in the spin-down ($\Omega = \Lambda - \frac{1}{2}$) dominant one-quasiparticle states [2,11]; a particle-rotor model calculation gave a similar result [12]. On the other hand, the counterpart, i.e., the spin-up ($\Omega = \Lambda + \frac{1}{2}$) dominant configurations showed almost no signature dependence of $B(M1)$ values, which is consistent with expectations given by the cranking model [13]. In order to clarify the general feature in this mass region, the intermediate situation in which the spin-down and spin-up configurations are strongly mixed should be studied. In this paper we present the results of Coulomb-excitation experiments on ^{155,157}Gd whose ground states contain comparable magnitudes of the spin-down and spin-up configurations. Part of this work has been published elsewhere [14].

Since the natural-parity rotational bands are generally nonyrast at high spins, they have not been well studied through in-beam γ-ray spectroscopy using heavy-ion-induced fusion reactions. Coulomb excitation is most suited for this study because the ground-state rotational band is selectively excited even if it is a nonyrast band. We made multiple Coulomb excitations of ^{155,157}Gd whose ground-state rotational bands are commonly based on the natural-parity Nilsson state $\nu[521\frac{3}{2}]$. We have assigned levels up to $J^\pi = (\frac{25}{2}^-)$ in ^{155}Gd and $J^\pi = \frac{25}{2}^-$ in ^{157}Gd. We measured γ-ray branchings, $E2/M1$ mixing ratios, and nuclear lifetimes and determined the absolute intraband transition probabilities up to the $\frac{21}{2}^-$ state in ^{155}Gd and the $\frac{23}{2}^-$ state in ^{157}Gd . The ground-band members of ^{155}Gd have previously been assigned up to $(\frac{15}{2})^-$. The absolute transition probabilities have been investigated through β^- decay [15] and Coulomb excitation by light ions [16–20]. Similarly, the ground-band members of ^{157}Gd have been established up to $J^\pi = \frac{15}{2}^-$ [21], and the transition probabilities have been determined up to the second excited $\frac{7}{2}^-$ state through β^- decay [22] and Coulomb excitation [23].

II. EXPERIMENTAL PROCEDURES AND RESULTS

Self-supporting metallic targets of ^{155}Gd (91.8 % enriched) and ^{157}Gd (93.3 % enriched) were bombarded with beams of 240-MeV ^{58}Ni and 305-MeV ^{81}Br from the tandem accelerator at Japan Atomic Energy Research Institute (JAERI). In Coulomb excitation of these nuclei, we performed γ-γ coincidence, γ-ray angular distribution

and recoil-distance lifetime measurement for the two nuclei. In the γ-γ coincidence and γ-ray angular distribution experiment for ^{157}Gd the ^{81}Br beam was used; The ^{58}Ni beam was used for all the other studies. In the γ-γ coincidence and γ-ray angular distribution measurement, the beam was stopped in the target with 30 mg/cm^2 thickness.

Three Compton-suppression γ-ray spectrometers [24] placed at 0°, 90°, and −90° to the beam direction were used in the γ-γ coincidence measurement. The distance between the target and the detectors was 7 cm. The data acquisition was controlled by a VAX-780 computer and all events were recorded on magnetic tapes for later analysis. The sums of the coincidence spectra gated for ground-band transitions are shown in Figs. 1(a) and 1(b) for ^{155}Gd and ^{157}Gd, respectively. Levels up to 1809 keV in ^{155}Gd and to 1630 keV in ^{157}Gd were determined from the coincidence spectra. The results are shown in Figs. 2(a) and 2(b).

Gamma-ray angular distributions were measured with a Compton- suppression spectrometer at seven angles between 0° and 90° to the beam direction. The distance between the target and the spectrometer was 10 cm. The angular distribution $W(\theta)$ was expanded to fourth order in Legendre polynomials

$$W(\theta) = A_0[1 + A_2Q_2P_2(\cos\theta) + A_4Q_4P_4(\cos\theta)] \quad . \tag{1}$$

The coefficients A_2 and A_4 were determined by fitting the experimental data. The Q_2 and Q_4 values are the geometrical attenuation factors. For the detector configuration used, the Q_2 and Q_4 were estimated for each γ-ray energy from Ref. [25]. Typical examples of the angular distribution analysis are shown in Fig. 3 and the derived coefficients A_2 and A_4 are presented in Tables I and II. We also evaluated the alignment attenuation factors [26], α_2 and α_4 : The experimental A_2 values of the $\Delta I = 2$ transitions give the alignment attenuation factor, α_2, for the decaying states because these transitions are pure $E2$; α_4 was estimated from the α_2 by assuming a Gaussian distribution of the magnetic-substate popula-

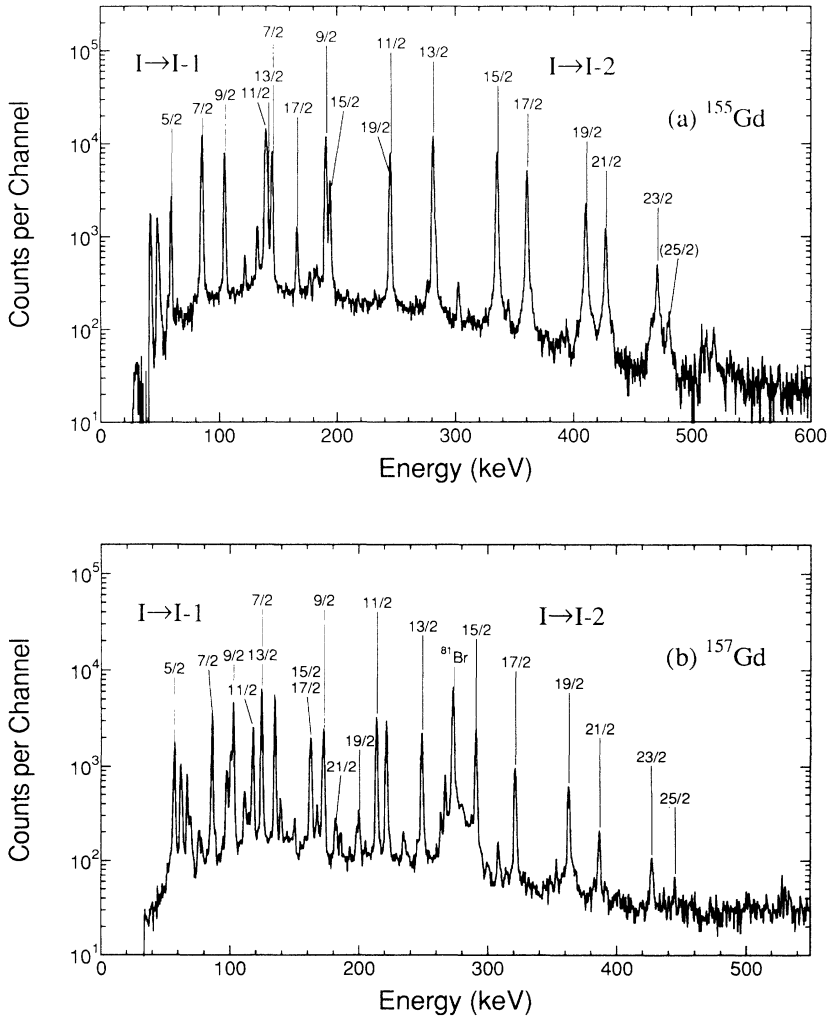

FIG. 1. Sum of coincidence spectra gated for ground-band transitions for (a) ^{155}Gd and (b) ^{157}Gd. Beams of 240-MeV ^{58}Ni and 305-MeV ^{81}Br were used to Coulomb excite the ^{155}Gd and ^{157}Gd nuclei, respectively.

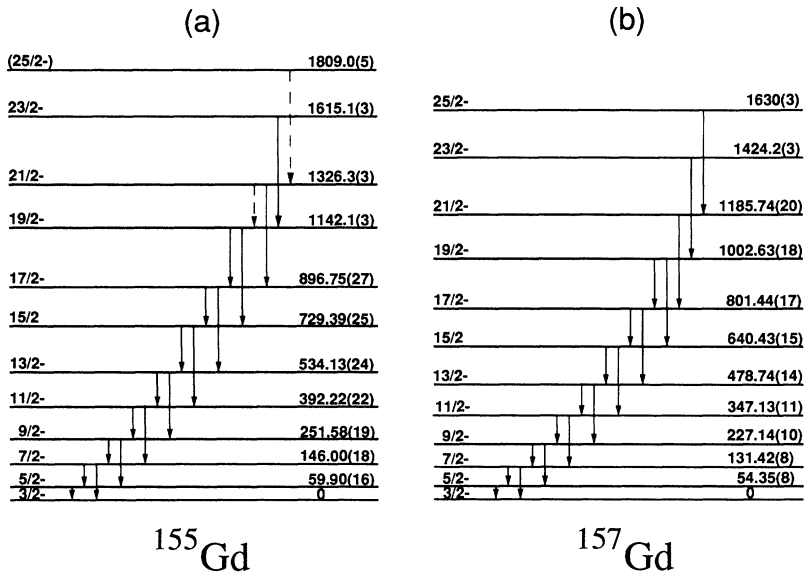

FIG. 2. Level schemes of the ground-state rotational bands of (a) ^{155}Gd and (b) ^{157}Gd. Level energies are determined by fitting transition energies given in Tables I and II.

tion. An $E2/M1$ mixing ratio for a $\Delta I = 1$ transition is derived from the attenuation factors for the state of interest and the angular distribution coefficients. The γ-ray intensities derived from the γ-ray angular-distribution analyses for ^{155}Gd and ^{157}Gd are presented in Tables I and II, respectively.

Lifetime measurement was made by the Doppler-shift recoil-distance method. In this case, the target thicknesses of ^{155,157}Gd were 2.9 and 3.9 mg/cm^2, respectively. Back-scattered projectiles were measured with a plastic annular scintillator which subtended an angle range of $\theta_{\rm lab} = 150°$–$175°$ to the beam direction. Gamma-rays in coincidence with the back-scattered projectiles were measured with a Compton-suppression γ-ray spectrometer placed at 0° to the beam direction. The distance between the target and the spectrometer was 13 cm. The average value of the recoil velocity was determined from the positions of shifted and unshifted γ-ray peaks: $(0.040\pm0.002)c$ for ^{155}Gd and $(0.035\pm0.003)c$ for ^{157}Gd, where c is the velocity of light. The coincidence spectra were measured for twelve recoil distances ranging from 15 μm to 8.28 mm. The electric pulse height, which re-

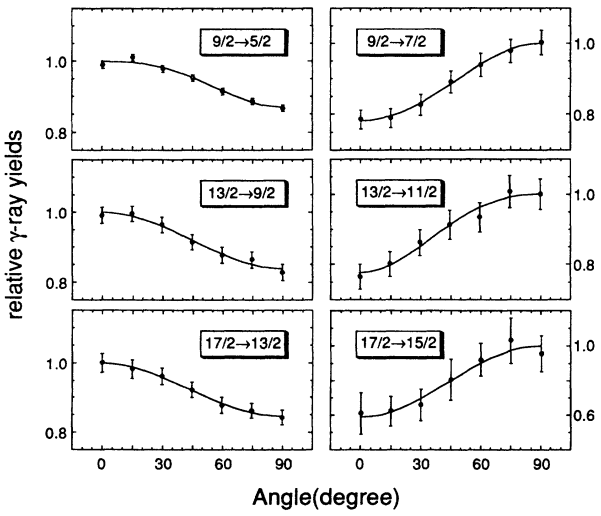

FIG. 3. Typical examples of γ-ray angular-distribution analysis for ^{155}Gd.

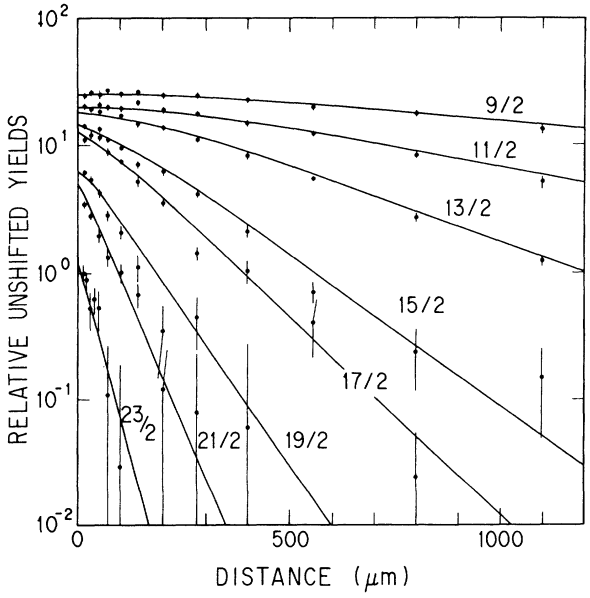

FIG. 4. Decay curves for the ground-band members of ^{157}Gd. The intensities were summed for $\Delta I = 1$ and $\Delta I = 2$ transitions depopulating each state.

TABLE I. Summary of γ transitions in the ground-state rotational band of ^{155}Gd. E_γ is γ-ray energy. J_i and J_f are initial and final spin, respectively. I_γ denotes the relative γ-ray intensity which is corrected for angular distributions; the data up to $J_i = \frac{11}{2}$ are derived from Ref. [20]. $I_{\rm total}$ indicates the total intensity corrected for internal conversions. A_2 and A_4 are γ-ray angular-distribution coefficients. $\delta(E2/M1)$ is the $E2/M1$ mixing ratio. Values in parentheses denote uncertainties.

J_i	J_f	E_γ (keV)	I_γ	$I_{\rm total}$	A_2	A_4	$\delta(E2/M1)$
$\frac{5}{2}$	$\frac{3}{2}$	60.0(1)	100(2)	1036(20)	-0.10(6)	0.13(6)	-0.197(5)[a]
$\frac{7}{2}$	$\frac{5}{2}$	86.1(1)	75.1(24)	320(10)	-0.044(33)	0.00(4)	$\pm$0.19(4)[b]
$\frac{7}{2}$	$\frac{3}{2}$	146.1(1)	24.9(2)	41(4)	0.007(22)	-0.005(27)	
$\frac{9}{2}$	$\frac{7}{2}$	105.4(1)	48(4)	132(11)	-0.160(27)	0.006(31)	-0.22(5)
$\frac{9}{2}$	$\frac{5}{2}$	191.5(1)	52(4)	66(5)	0.102(19)	-0.019(24)	
$\frac{11}{2}$	$\frac{9}{2}$	140.0(1)	41(7)	73(12)	-0.221(25)	-0.013(28)	-0.32(5)
$\frac{11}{2}$	$\frac{7}{2}$	245.5(1)	59(7)	65(8)	0.125(19)	-0.010(24)	
$\frac{13}{2}$	$\frac{11}{2}$	142.0(1)	8.9(27)	9.1(28)	-0.150(35)	-0.024(40)	-0.14(4)
$\frac{13}{2}$	$\frac{9}{2}$	282.0(1)	58(3)	58(3)	0.121(19)	-0.002(24)	
$\frac{15}{2}$	$\frac{13}{2}$	194.9(1)	8.8(27)	8.9(27)	-0.164(20)	0.025(23)	-0.13(5)
$\frac{15}{2}$	$\frac{11}{2}$	336.9(1)	31(13)	31(13)	0.108(19)	0.008(24)	
$\frac{17}{2}$	$\frac{15}{2}$	166.6(1)	1.2(3)	1.2(3)	-0.31(9)	-0.01(11)	-0.15(4)
$\frac{17}{2}$	$\frac{13}{2}$	361.5(1)	15.5(9)	15.5(9)	0.114(20)	0.002(24)	
$\frac{19}{2}$	$\frac{17}{2}$	244.4(1)	0.9(6)	0.9(6)	-0.402(12)	0.031(16)	-0.20(4)
$\frac{19}{2}$	$\frac{15}{2}$	411.0(1)	5.0(21)	5.0(21)	0.111(23)	-0.010(29)	
$\frac{21}{2}$	$\frac{17}{2}$	427.7(1)	1.8(6)	1.8(6)	0.112(39)	0.027(49)	
$\frac{23}{2}$	$\frac{19}{2}$	473.(1)	-	-	-	-	
$(\frac{25}{2})$	$\frac{21}{2}$	483.(2)	-	-	-	-	

[a]From Refs. [16, 17].
[b]From Ref. [18].

flects the capacitance between the target and stopper, was monitored during the measurements.

Figure 4 shows the unshifted intensity versus the recoil distance, i.e., decay curves for excited states. Data on the shifted and unshifted intensities were analyzed by a computer program LIFETIME [27]. The fitted results are also shown in Fig. 4. The Coulomb-excitation process does not cause any serious side-feeding contribution to the decay curves which often brings considerable uncertainty of the final result in compound nuclear residues. This feature enables the lifetimes of excited states to be determined accurately.

The lifetimes obtained for the states in ^{155}Gd and ^{157}Gd, and the reduced $M1$ and $E2$ transition probabilities derived from the γ-ray intensities, $E2/M1$ mixing ratios, and lifetimes are summarized in Table III. The reduced transition probabilities are plotted in Figs. 5–7.

III. THEORETICAL CALCULATION

We performed cranking-model calculation based on the Nilsson potential. In this framework, all the single-particle states in the model space are treated on the same footing, and no *a priori* assumption for the core is necessary. In particular, our $M1$ matrix elements are not just multiples of angular-momentum matrix elements in contrast to the single-j approximation; this feature is essential for studying natural-parity rotational bands. And our $B(E2)$ values are calculated using the microscopic

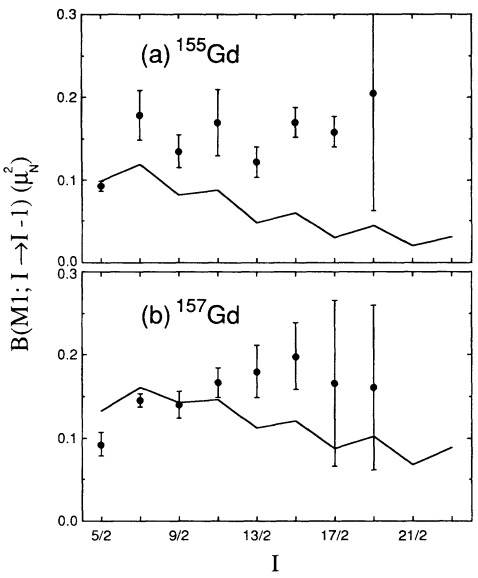

FIG. 5. $B(M1; I \rightarrow I-1)$ values for the ground-state rotational bands of (a) ^{155}Gd and (b) ^{157}Gd. The experimental values for $I = \frac{5}{2}$ and $\frac{7}{2}$ are previous data (see Table III), and the others the present data. The solid line shows the cranking-model calculation.

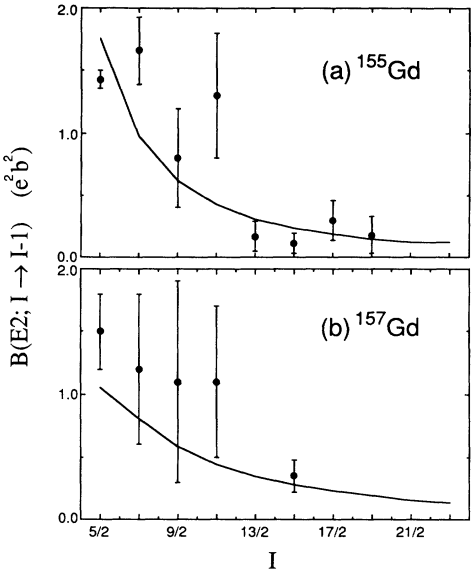

FIG. 6. $B(E2; I \rightarrow I-1)$ values for the ground-state rotational bands of (a) ^{155}Gd and (b) ^{157}Gd. The experimental values for $I = \frac{5}{2}$ and $\frac{7}{2}$ are previous data (see Table III), and the others the present data. The solid line denotes the present cranking-model calculation.

expectation value of the quadrupole moment at each rotational frequency. Electromagnetic transition operators we study are given by [28]

$$\mu_{-1} = [1-(K/I)^2]^{1/2}[(g_\ell - g_{\rm ref})\ell_{-1}^{(\rm odd)} + (g_s^{(\rm eff)} - g_{\rm ref})s_{-1}^{(\rm odd)}] \quad ,$$
$$Q_{2-1} = -i[1-(K/I)^2]^{1/2}(\frac{3}{2})^{1/2}\langle Q_0\rangle J_z^{(\rm odd)}/I_0 \quad , \qquad (2)$$
$$Q_{2-2} = -[1-(K/I)^2](\frac{3}{8})^{1/2}\langle Q_0\rangle$$

for axially symmetric odd-N nuclei. The first factor in each operator is the geometrical factor proposed by Dönau [29] to improve the cranking approximation for the low-spin region (see appendix in Ref. [13]). In the present case, $K = \frac{3}{2}$ was assumed. In the $M1$ operator, $g_{\rm ref}$ is calculated using the microscopic expectation values with respect to the even-even reference state as

$$g_{\rm ref} = \frac{\langle \mu_x\rangle}{\langle J_x\rangle} \quad . \qquad (3)$$

The effective spin g factor was taken from Table 5-14 in Ref. [30] and no effective charge was introduced. The quantity I_0 is the angular momentum of the even-even reference state and is assumed to be related to the odd-mass system quantities as

$$I_0 = \langle J_x\rangle = I - i_x \quad , \qquad (4)$$

where i_x is the aligned angular momentum of the odd quasiparticle.

Wave functions on which the above operators act were obtained by diagonalizing

$$h' = h_{\rm Nils} - \Delta(P^\dagger + P) - \lambda N - \hbar\omega_{\rm rot}J_x \qquad (5)$$

in a three-major-shell space which consists of the $N_{\rm osc} =$ 4–6 shells for neutrons and the $N_{\rm osc} =$ 3–5 shells for protons. By assuming axial symmetry, the quadrupole deformation parameter δ was chosen so as to reproduce

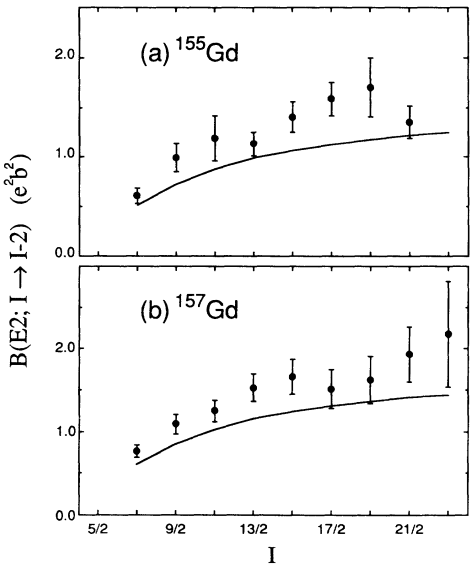

FIG. 7. $B(E2; I \rightarrow I-2)$ values for the ground-state rotational bands of (a) ^{155}Gd and (b) ^{157}Gd. The experimental values for $I = \frac{7}{2}$ are previous data (see Table III), and the others the present data. The solid line denotes the present cranking-model calculation.

TABLE II. Summary of γ transitions in the ground-state rotational band of ^{157}Gd. Notations are the same as those in Table I. Gamma-ray branching ratio for $J_i = \frac{7}{2}$ is from Ref. [21].

J_i	J_f	E_γ (keV)	I_γ	I_{total}	A_2	A_4	$\delta(E2/M1)$
$\frac{5}{2}$	$\frac{3}{2}$	54.4(1)	100(2)	1340(50)	-	-	-0.182(12)[a]
$\frac{7}{2}$	$\frac{5}{2}$	77.1(1)	100	544	-0.052(9)	0.084(13)	-0.18(3)[a]
$\frac{7}{2}$	$\frac{3}{2}$	131.4(1)	30.0(25)[b]	59(5)	(-0.110(9)	0.020(11))	
$\frac{9}{2}$	$\frac{7}{2}$	95.8(1)	32.4(6)	109(2)	-0.0153(9)	-0.016(11)	-0.22(9)
$\frac{9}{2}$	$\frac{5}{2}$	172.8(1)	29.4(10)	40.2(14)	0.099(9)	0.031(12)	
$\frac{11}{2}$	$\frac{9}{2}$	120.1(1)	19.5(4)	44.0(9)	-0.228(9)	-0.013(12)	-0.25(7)
$\frac{11}{2}$	$\frac{7}{2}$	215.6(1)	25.9(5)	30.5(6)	0.134(9)	0.010(12)	
$\frac{13}{2}$	$\frac{11}{2}$	131.6(1)	6.3(7)[b]	9.1(28)	(-0.110(9)	0.020(11))	-
$\frac{13}{2}$	$\frac{9}{2}$	251.6(1)	15.5(3)	17.2(3)	0.206(9)	-0.023(12)	
$\frac{15}{2}$	$\frac{13}{2}$	161.7(1)	3.6(6)[b]	5.5(9)	-0.371(9)	-0.009(12)	-0.18(3)
$\frac{15}{2}$	$\frac{11}{2}$	293.3(1)	10.3(5)	11.0(5)	0.235(8)	-0.042(12)	
$\frac{17}{2}$	$\frac{15}{2}$	161.0(1)	1.0(4)[b]	1.5(6)	-	-	-
$\frac{17}{2}$	$\frac{13}{2}$	322.7(1)	5.17(28)	5.42(29)	0.284(8)	-0.047(12)	
$\frac{19}{2}$	$\frac{17}{2}$	201.(1)	0.39(23)	0.5(3)	-	-	-
$\frac{19}{2}$	$\frac{15}{2}$	362.2(1)	1.99(13)	2.06(13)	0.294(14)	-0.077(18)	
$\frac{21}{2}$	$\frac{19}{2}$	195(1)	-	-	-	-	-
$\frac{21}{2}$	$\frac{17}{2}$	384.3(1)	0.51(10)	0.52(10)	-	-	
$\frac{23}{2}$	$\frac{19}{2}$	422(1)	0.09(5)	0.09(5)	-	-	
$\frac{25}{2}$	$\frac{21}{2}$	444(3)	-	-	-	-	

[a]From Ref. [21].
[b]Composite peak. The γ-ray intensity is derived from analysis of γ-γ coincidence measurements; The effect of angular correlation is corrected.

the observed quadrupole moments of the adjacent even-even nuclei [31] approximately using experimental pairing gaps and the chemical potentials which gave the correct particle numbers at $\hbar\omega_{\text{rot}} = 0$. The parameters used are listed in Table IV.

In the next section, we shall present new calculated results for ^{157}Gd as well as the previous results for ^{155}Gd [11], and compare them with our new experimental data.

IV. DISCUSSION

A. Theoretical expectation

Both the single-particle angular momentum **J** and the magnetic dipole operators $\boldsymbol{\mu}$ are given by linear combinations of $\boldsymbol{l}$ and **s**. In the single-j approximation, the matrix elements of J_ν and μ_ν ($\nu = -1, 0, +1$) are proportional to each other:

$$\mu_{-1} = (g_j - g_{\text{ref}})J_{-1} \quad , \tag{6}$$

where g_j is the Schmidt value defined by using $g_s^{(\text{eff})}$, because the relation between j and l is unique. This is well applied to high-j intruder orbitals. In natural-parity cases, however, j is not a good quantum number in the deformed nuclei.

By assuming axial symmetry, an identity

$$-\Delta e' \langle f|J_z|u\rangle = \hbar\omega_{\text{rot}} \langle f|iJ_y|u\rangle \quad , \tag{7}$$

where

$$\begin{aligned} &\Delta e' = e'_u - e'_f > 0 \quad , \\ &h'|f\rangle = e'_f|f\rangle \quad , \\ &h'|u\rangle = e'_u|u\rangle \end{aligned} \tag{8}$$

TABLE III. Summary of lifetimes and reduced transition probabilities for ^{155,157}Gd. I is nuclear spin. τ is mean lifetime.

Nucleus	I	τ (ps)	$B(E2; I \to I-2)$ (e^2b^2)	$B(M1; I \to I-1)$ (μ_N^2)	$B(E2; I \to I-1)$ (e^2b^2)
^{155}Gd	$\frac{5}{2}$	270(14)[a]		0.092(6)[b]	1.43(7)[c]
	$\frac{7}{2}$	390(70)[a]	0.61(8)[c]	0.18(3)[d]	1.66(27)[d]
	$\frac{9}{2}$	84(9)	1.00(15)	0.134(20)	0.8(4)
	$\frac{11}{2}$	33(3)	1.19(23)	0.17(4)	1.3(5)
	$\frac{13}{2}$	32(3)	1.13(12)	0.122(13)	0.17(12)
	$\frac{15}{2}$	10.3(11)	1.40(15)	0.170(18)	0.11(8)
	$\frac{17}{2}$	7.5(8)	1.59(17)	0.159(19)	0.30(16)
	$\frac{19}{2}$	3.4(4)	1.7(3)	0.20(14)	0.18(15)
	$\frac{21}{2}$	4.2(5)	1.35(17)	-	-
^{157}Gd	$\frac{5}{2}$	188(12)[e]		0.090(7)[b]	1.47(7)[c]
	$\frac{7}{2}$	137(7)[e]	0.61(5)[c]	0.146(8)[d]	1.2(6)[d]
	$\frac{9}{2}$	24.1(21)	1.09(12)	0.140(16)	1.1(8)
	$\frac{11}{2}$	17.6(15)	1.25(13)	0.167(18)	1.1(6)
	$\frac{13}{2}$	10.6(9)	1.53(17)	0.180(31)[f]	-
	$\frac{15}{2}$	6.2(5)	1.66(21)	0.20(4)	0.35(13)
	$\frac{17}{2}$	3.7(3)	1.51(23)	0.17(10)	-
	$\frac{19}{2}$	2.61(23)	1.62(28)	0.16(10)	-
	$\frac{21}{2}$	1.66(24)	1.9(3)	-	-
	$\frac{23}{2}$	0.86(7)	2.2(6)	-	-

[a]From Ref. [20].
[b]Deduced from $B(E2; I \to I-1)$ and $\delta(E2/M1)$.
[c]From Ref. [19].
[d]Deduced from τ and branching and mixing ratios.
[e]From Ref. [21].
[f]Deduced by assuming $\delta(E2/M1) = -0.20 \pm 0.20$, which well covers all the $\delta(E2/M1)$ values measured for ^{157}Gd (see Table II).

can be derived from a commutation relation $[h', J_z]$ (Ref. [32]). Here $|f\rangle$ and $|u\rangle$ denote intrinsic favored and unfavored signature states, respectively; each signature corresponds to either of $+i$ or $-i$ depending on the angular momentum of a dominant single-particle orbital. The signature dependence of $B(M1)$ is determined by the relative sign between the matrix elements of $i\mu_y$ and μ_z in Eq. (9).

$$B(M1; f \rightleftarrows u) = \frac{1}{2}|\langle f|\mu_z|u\rangle \mp \langle f|i\mu_y|u\rangle|^2 \qquad (9)$$

$B(M1; f \to u)$ is always larger than $B(M1 : u \to f)$ according to the identity (7) when axial symmetry and the proportionality between $\boldsymbol{\mu}$ and $\mathbf{J}$ are fulfilled. This proportionality does not hold in the natural-parity cases because many spherical components with different j are included in natural-parity deformed orbitals, and consequently the signature dependence can be inverted due to cancellation between the orbital and the spin contributions.

The necessary conditions for the occurrence of this inversion were clarified in Ref. [11]: There it is shown that the inversion occurs when

$$\frac{\langle f|i\mu_y|u\rangle\langle f|J_z|u\rangle}{\langle f|\mu_z|u\rangle\langle f|iJ_y|u\rangle} < 0 \quad . \qquad (10)$$

TABLE IV. Parameters used in the cranking-model calculation. δ is deformation parameter.

Nucleus	δ	Δ_n (MeV)	Δ_p (MeV)	$g_s^{(\mathrm{eff})}/g_s^{(\mathrm{free})}$	i_x
^{155}Gd	0.26	1.05	1.05	0.79	1.3
^{157}Gd	0.28	0.94	0.93	0.87	0.8

The following two conditions must be fulfilled to satisfy inequality in expression (10):

$$\frac{\langle f|is_y|u\rangle}{\langle f|il_y|u\rangle} \neq \frac{\langle f|s_z|u\rangle}{\langle f|l_z|u\rangle} \tag{11}$$

and

$$\frac{g_s^{(\mathrm{eff})} - g_{\mathrm{ref}}}{g_l - g_{\mathrm{ref}}} \lessgtr 0 \quad \text{for} \quad \Omega = \Lambda \mp \frac{1}{2} \quad . \tag{12}$$

Although both the spin-down and spin-up components are contained in actual natural-parity orbitals, dominant components can be deduced from studies of the quasiparticle energies. A prediction was made for the $[521\frac{3}{2}]$ band of ^{155}Gd in Ref. [11]. This orbital contains both the $\Omega = \Lambda - \frac{1}{2}$ and $\Omega = \Lambda + \frac{1}{2}$ components in comparable magnitudes. But the spin-down character becomes dominant in the high spin region, indicating that the favored (unfavored) signature is $-i$ $(+i)$. This may be attributed to the fact that the Coriolis interaction is strongest in the $h_{9/2}$ component among the natural-parity components included. The prediction is that, on the assumption that the nuclear shape is axially symmetric, $B(M1; u \rightarrow f)$ will be larger than $B(M1; f \rightarrow u)$ in the one-quasiparticle band, which is apparently in disagreement with the selection rule in the single-j model [3].

B. Characteristics of the experimental data

Electromagnetic transition rates as well as quasiparticle energy splittings in the $[521\frac{3}{2}]$ bands of ^{155}Gd and ^{157}Gd are shown in Figs. 5–8. The experimental signature splittings $\Delta e' = e'_{+i} - e'_{-i}$ are shown by solid lines in Fig. 8. Their sign is consistent with the dominant $h_{9/2}$ character. Their magnitudes in ^{157}Gd are about one half of those in ^{155}Gd. This difference can be understood, at least qualitatively, as due to the difference in the nuclear deformation δ. The $B(M1)$ values are shown in Fig. 5. A distinct neutron-number dependence can be found in this quantity: (a) the signature-averaged magnitudes are almost independent of spin in ^{155}Gd, while they increase gradually as a function of spin in ^{157}Gd; (b) the inverted signature dependence occurs in ^{155}Gd but it is not clearly seen in ^{157}Gd. The $B(E2)$ values with $\Delta I = 1$ and 2 are shown in Figs. 6 and 7. They are rather smooth functions of spin. The uncertainties in the $B(E2; I \rightarrow I-1)$ values are, unfortunately, too large to allow any conclusions to be drawn from these data.

Measured $B(M1)$ values in the natural-parity ground-state bands of ^{163}Dy [2], ^{173}Yb [13], and ^{155}Gd [present study] are compared in Fig. 9. ^{163}Dy and ^{173}Yb correspond to dominant $h_{9/2}$ (spin-down) and $f_{7/2}$ (spin-up) bands, respectively, whereas the ^{155}Gd stands for the case in which these components are strongly mixed. There is an interesting systematic feature: the signature-averaged magnitudes of $B(M1)$ become smaller and the inverted signature dependence becomes more conspicuous as the spin-down components stemming from the $h_{9/2}$ orbitals in the wave function become dominant. The first feature is due to the sign of g_j : since it is negative for $f_{7/2}$ whereas positive for $h_{9/2}$ and g_{ref} is positive for 1qp (one-quasiparticle) bands, a cancellation in $B(M1)$, which is proportional to $(g_j - g_{\mathrm{ref}})^2$ in their partial contributions, occurs in the case of $h_{9/2}$.

C. Comparison between experimental and theoretical results

Results of theoretical calculations for ^{155}Gd and ^{157}Gd are presented in Figs. 5–8 along with the experimental data. The signature splittings $\Delta e'$ in ^{155}Gd are reproduced excellently by the calculation using an axially symmetric shape deduced from the measured quadrupole

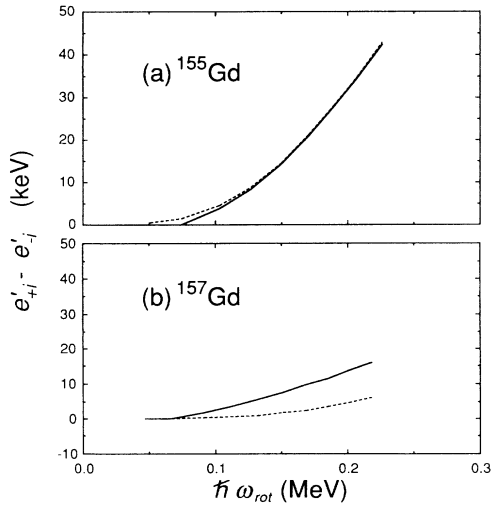

FIG. 8. Quasiparticle energy splittings of the ground-state rotational bands in (a) ^{155}Gd and (b) ^{157}Gd. The solid line connects the experimental values. The dashed line shows the calculation.

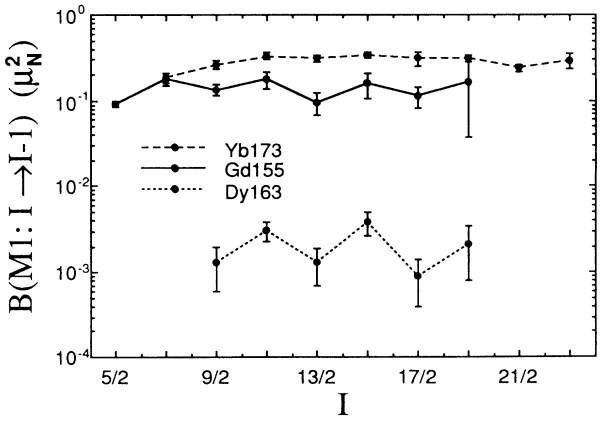

FIG. 9. Comparison of experimental $B(M1)$ values of three natural-parity rotational bands. The upper, middle and lower ones correspond to ^{173}Yb, ^{155}Gd and ^{163}Dy, respectively. Three kinds of lines connecting the experimental values are shown to guide the eye. The absolute $B(M1)$ values of ^{157}Gd are close to those of ^{155}Gd and are omitted in this figure.

moments of the adjacent even-even nuclei. In ^{155}Gd signature dependence of $B(M1)$ is seen in the calculation as well as in the experiment although the measured absolute values are not well reproduced by the calculation.

In ^{157}Gd, the calculation gives a similar result to that of ^{155}Gd: The sign of the quasiparticle energy splittings is the same and the inverted signature dependence of $B(M1)$ are seen. However, the energy splittings calculated in the same way as in ^{155}Gd are twice as small as the corresponding experimental values. The calculation for $B(M1)$ deviates from the experimental values at high spins, giving smaller values. The origin of this difference is not clear. Although we examined the effects of the γ degree of freedom, we did not improve the results unlike the case of ^{163}Dy.

$B(E2; I \rightarrow I-2)$ values are almost independent of the neutron number in both the experiment and calculation. The calculated values, however, are systematically smaller than the experiment. Since the quadrupole deformation is derived from the experimental quadrupole moments of adjacent even-even nuclei, the deviation may indicate that the deformation of ^{155,157}Gd is larger than the even-even nuclei. This indication, however, contradicts the observation of quasiparticle energy splitting because the larger deformation causes smaller energy splitting and results in larger deviation from the experiment. $B(E2; I \rightarrow I-1)$ values in ^{155}Gd and ^{157}Gd are reproduced within the experimental accuracy.

V. SUMMARY

We have studied experimentally and theoretically the electromagnetic transition properties as well as the energy spectra of the natural-parity ground-state rotational bands of ^{155}Gd and ^{157}Gd. We paid special attention to the inverted signature dependence of $B(M1)$ with respect to the sign of quasiparticle energy splitting $\Delta e'$ that was found [2] in ^{163}Dy, and was predicted [11] for ^{155}Gd in terms of the cranking model. By comparing the present results especially for ^{155}Gd with those for ^{163}Dy and ^{173}Yb which were previously reported [2,13], it is found that there is an interesting systematic behavior in $B(M1)$: the signature-averaged magnitude becomes smaller and the (inverted) signature dependence becomes more conspicuous as the spin-down components increase. The predicted inverted signature dependence of $B(M1)$ for ^{155}Gd has been verified by the experiment. A new calculation performed for ^{157}Gd in the same way as that for ^{155}Gd showed a result similar to that for ^{155}Gd and reproduced gross features of the experimental results, i.e., the sign of $\Delta e'$ and the signature dependence of $B(M1)$ at low spins. The $B(M1)$ values of ^{157}Gd tend to deviate from the calculation at high spins. The source of this deviation has not been found. As for $B(E2)$ values of both nuclei, the experimental trend as a function of spin is reproduced well by the theoretical calculation.

ACKNOWLEDGMENTS

We would like to thank Dr. M. Ishii at JAERI and Dr. H. Kamitsubo at RIKEN for their support of this study. We also thank Dr. P. Möller for reading the manuscript. This study has been carried out as a joint research program between JAERI and RIKEN.

[1] E. Minehara, M. Oshima, S. Kikuchi, T. Inamura, A. Hashizume, and H. Kumahora, Phys. Rev. C **35**, 858 (1987).

[2] M. Oshima, E. Minehara, S. Kikuchi, T. Inamura, A. Hashizume, H. Kusakari, and M. Matsuzaki, Phys. Rev. C **39**, 645 (1989).

[3] I. Hamamoto, Phys. Lett. **106B**, 281 (1981); in *Proceedings of the Niels Bohr Centennial Conference on Nuclear Structure*, Copenhagen, 1985, edited by R. Broglia, G.B. Hagemann, and B. Herskind (North-Holland, Amsterdam, London, 1985), p. 129.

[4] G.B. Hagemann, J.D. Garrett, B. Herskind, J. Kownacki, B.M. Nyakó, P.L. Nolan, J.F. Sharpey-Schafer, and P.O. Tjøm, Nucl. Phys. **A424**, 365 (1984); D.C. Radford, H.R. Andrews, G.C. Ball, D. Horn, D. Ward, F. Banville, S. Flibotte, P. Taras, J. Johansson, D. Tucker, and J.C. Waddington, contributed to the Workshop on Nuclear Structure, The Niels Bohr Institute, 1988 (unpublished).

[5] M. Ohshima, E. Minehara, M. Ishii, T. Inamura, and A. Hashizume, Nucl. Phys. **A436**, 518 (1985).

[6] K. Honkanen, H.C. Griffin, D.G. Sarantites, V. Abenante, L.A. Adler, C. Baktash, Y.S. Chen, O. Dietzsch, M.L. Halbert, D.C. Hensley, N.R. Johnson, A.J. Larabee, I.Y. Lee, L.L. Riedinger, J.X. Saladin, T.M. Semkow, and Y. Schutz, in Proceedings of the American Chemical Society Meeting, 1986 (unpublished).

[7] J. Gascon, P. Taras, D.C. Radford, D. Ward, H.R. Andrews, and F. Banville, Nucl. Phys. **A467**, 539 (1987).

[8] C.-H. Yu, M.A. Riley, J.D. Garrett, G.B. Hagemann, J. Simpson, P.D. Forsyth, A.R. Mokhtar, J.D. Morrison, B.M. Nyakó, J.F. Sharpey-Schafer, and R. Wyss, Nucl. Phys. **A489**, 477 (1988).

[9] P. Frandsen, R. Chapman, J.D. Garrett, G.B. Hagemann, B. Herskind, C.-H. Yu, K. Schiffer, D. Klarke, F. Khazaie, J.C. Lisle, J.N. Mo, L. Carlén, P. Ekström, and H. Ryde, Nucl. Phys. **A489**, 508 (1988).

[10] M. Oshima, E. Minehara, S. Ichikawa, H. Iimura, T. Inamura, A. Hashizume, H. Kusakari, and S. Iwasaki, Phys. Rev. C **37**, 2578 (1988).

[11] M. Matsuzaki, Phys. Rev. C **39**, 691 (1989).

[12] A. Ikeda and T. Shimano, Prog. Theor. Phys. **85**, 547 (1991).

[13] M. Oshima, M. Matsuzaki, S. Ichikawa, H. Iimura, H. Kusakari, T. Inamura, A. Hashizume, and M. Sugawara, Phys. Rev. C **40**, 2084 (1989).

[14] M. Oshima and T.T. Inamura, in *Proceedings of the Second IN2P3-RIKEN Symposium on Heavy-ion Collisions,*

edited by B. Heusch and M. Ishihara (World Scientific, Singapore, 1990), p. 287.
[15] G. Lovhoiden, J.C. Waddington, K.A. Hagemann, S.A. Hjorth, and H. Ryde, Nucl. Phys. **A148**, 657 (1970).
[16] C. Foin, J. Oms, and J.-L. Barat, J. Phys. (Paris) **28**, 861 (1967).
[17] H.J. Krell and S. Hofmann, Z. Phys. A **272**, 257 (1975).
[18] A. Tveter and B. Herskind, Nucl. Phys. **A134**, 599 (1969).
[19] V. Ramsak, M.C. Olesen, and B. Elbek, Nucl. Phys. **6**, 451 (1958).
[20] M.A. Lee, Nucl. Data Sheets **50**, 563 (1987).
[21] R.L. Bunting and C.W. Reich, Nucl. Data Sheets **39**, 103 (1983); R.G.Helmer, *ibid.* **55**, 71 (1988).
[22] F. Sterba, P.O. Tjøm, and B. Elbek, Nucl. Phys. **A162**, 353 (1971).
[23] D.C. Tayal, K.P. Singh, and H.S. Hans, Phys. Rev. C **33**, 368 (1986).
[24] E. Minehara, M. Oshima, T. Inamura, A. Hashizume, and H. Kumahora, in Proceedings of the International Symposium on Nuclear Spectroscopy and Nuclear Interactions, Osaka, 1984 (unpublished).
[25] D.C. Camp and A.L. Van Lehn, Nucl. Instrum. Methods **76**, 192 (1969).
[26] H. Morinaga and T. Yamazaki, *In-Beam Gamma-Ray Spectroscopy* (North Holland, Amsterdam, 1976).
[27] J.C. Wells, M.P. Fewell, and N.R. Johnson, Oak Ridge National Laboratory Report No. ORNL/TM-9105, 1985.
[28] M. Matsuzaki, Y.R. Shimizu, and K. Matsuyanagi, Prog. Theor. Phys. **79**, 836 (1988).
[29] F. Dönau, Nucl. Phys. **A471**, 469 (1987).
[30] A. Bohr and B.R. Mottelson, *Nuclear Structure* (Benjamin, New York, 1975), Vol. 2.
[31] S. Raman *et al.*, At. Data Nucl. Data Tables **36**, 1 (1987).
[32] I. Hamamoto, Phys. Lett. **106B**, 281 (1981).